On the influence of the nozzle length on the arc properties in a cutting torch

2009 J. Phys.: Conf. Ser. 166 012021

(http://iopscience.iop.org/1742-6596/166/1/012021)

Journal of Physics: Conference Series **166** (2009) 012021 doi:10.1088/1742-6596/166/1/012021

On the influence of the nozzle length on the arc properties in a cutting torch

L Prevosto[1,†], H Kelly[2,‡], M Risso[1] and D Infante[1]

[1] Grupo de Descargas Eléctricas, Departamento Ingeniería Electromecánica, Universidad Tecnológica Nacional, Regional Venado Tuerto, Las Heras 644, Venado Tuerto (2600), Santa Fe, Argentina.
[2] Instituto de Física del Plasma (CONICET), Departamento de Física, Facultad de Ciencias Exactas y Naturales (UBA) Ciudad Universitaria Pab. I, (1428) Buenos Aires, Argentina

E-mail: prevosto@waycom.com.ar

Abstract. In this work, an experimental study on the influence of the nozzle geometry on the physical properties of a cutting arc is reported. Ion current signals collected by an electrostatic probe sweeping across a 30 A oxygen cutting arc at 3.5 mm from the nozzle exit were registered for different nozzle lengths. The temperature and density radial profiles of the arc plasma were found in each case by an inversion procedure of these signals. A comparison between the obtained results shows that the shorter nozzle (R_N = 0.50 mm, L_N = 4.5 mm operated at 0.7 MPa and 35 Nl/min) produces a thinner and hotter arc than the larger nozzle (R_N = 0.50 mm, L_N = 9.0 mm operated at 1.1 MPa and 20 Nl/min). This behavior is attributed to the marked difference of gas flow rate due to the clogging effect. A smaller gas mass flow reduces the convective cooling at the arc border and decreases the power dissipation of the arc column, resulting in small axis temperatures.

1. Introduction

Transferred arc plasma torches are widely used in industrial cutting process of metallic materials because of their ability to cut practically all metal and the high productivity than can be achieved with this technology. Plasma cutting is a process of metal cutting at atmospheric pressure by an arc plasma jet, where a transferred arc is generated between a cathode and a work-piece (the metal to be cut) acting as the anode. In order to obtain a high-quality cut, the arc must be as collimated as possible. To this end, a new generation of cutting torches, the so called “high energy density torch” or “high-definition torch” has been developed. These torches are characterized by an arc current intensity in the range of 30 ÷ 100 A, flat cathodes, oxygen as the plasma gas, very small nozzle diameters (≈ 1 mm) and by the generation of an under-expanded supersonic arc jet with a shock wave close to the nozzle exit [1].

Among the various possible ways of stabilizing an arc by a superimposed convective flow in a tube, gas vortex stabilization has been successfully used in cutting torches. In these torches the arc is

[†] Fellow of YPF
[‡] Member of the CONICET

confined to the center of the nozzle while an intense vortex of a gas is maintained at the arc periphery. Centrifugal forces drive the cold gas toward the walls, which is thus thermally well protected. In addition to the circumferential component of the vortex flow, there is also a superimposed axial velocity component that continuously supplies cold gas. The intense convective cooling produced at the arc border enhances the power dissipation in the arc column, which, in turn, results in high axis temperatures [2]. Due to the clogging effect of the heated gas in the nozzle [3], the gas mass flow rate is typically small and the level of stabilization of the arc may be insufficient to avoid double-arcing problems (where the arc is split into two: one connecting the cathode and the nozzle, the other connecting the nozzle and work piece). This phenomenon is one of the main drawbacks that put a limit to increasing capabilities of plasma arc cutting process [4]. An optimal design of a cutting torch nozzle must satisfy contradictory conditions. In order to provide a fast, highly constricted and hot plasma jet, the nozzle should be long and narrow. On the other hand, such long and narrow nozzle reduces the gas mass flow, with the consequent de-stabilization and asymmetry of the arc. Differences in cutting arc properties related to changes in the nozzle radius were measured using spectroscopic techniques in [5].

In this work, an experimental study on the influence of the nozzle length on the physical properties of a cutting arc is reported. Ion current signals collected by an electrostatic probe sweeping across a 30 A oxygen cutting arc at 3.5 mm from the nozzle exit for two different nozzle lengths was registered. The temperature and density radial profiles of the arc plasma were obtained in each case by an inversion procedure of these signals. A comparison between the results obtained for both nozzle lengths is presented and discussed.

2. Experiment

The cutting torch used in this study consisted of a cathode centered above an orifice in a converging-straight copper nozzle with liquid cooling. The cathode was made of copper (7 mm in diameter) with a hafnium tip (1.5 mm in diameter) inserted at the cathode center. A flow of oxygen gas cooled the cathode and was also employed as the plasma gas. The gas passed through a swirl ring to provide arc stability. Two converging-straight bore nozzle designs were used and compared. In both cases the bore radius of the nozzle cylindrical part was R_N = 0.5 mm whereas its length presented a marked difference L_N = 4.5 and 9 mm.

To avoid plasma contamination by metal vapors from the anode, a rotating steel disk with 200 mm in diameter and 15 mm thickness was used as the anode [3]. In this study, the disk upper surface was located at 5 mm from the nozzle exit. The arc was transferred to the edge of the disk, and the rotating frequency of the disk was equal to 29.5 Hz. At this velocity, a well-stabilized arc column was obtained, and no noticeable damage on the lateral surface of the anode disc was found. Thus, practically no metal vapors from the anode were present in the arc. A scheme of the torch indicating several geometric dimensions of the nozzle is presented in Fig. 1.

During arc operation the total arc voltage (V_{CA}) and the nozzle floating voltage (V_{NA}) were registered with respect to the grounded anode, either by using a high-impedance (10 MΩ) voltage meter or by registering them on a digitizing oscilloscope. By performing a small orifice (1 mm in diameter) on the cathode lateral surface the pressure in the plenum chamber (p_{ch}) was measured by connecting a pressure meter at the upper head of the cathode. The gas flow rate injected in the torch was also registered. In this experiment, the arc current was fixed to a value of 30 A.

The electrostatic probe system employed for studying the arc was similar to that previously reported in [6] and consisted of a thin tungsten wire with a radius R_p = 0.1 mm, sweeping trough an arc plane perpendicular to the current flow direction at a constant velocity v_p = 18 m s^{-1}. Since an arc cutting torch creates an under-expanded sonic flow at the nozzle exit, we studied the arc plane at z = 3.5 mm (where z is the axial position measured from the nozzle exit). At this axial position the arc pressure p can be considered to be near to the atmospheric value [1]. A scheme of the probe circuit is also shown in Fig. 1. To obtain ion current measurements, the probe was biased with a resistance (R_1 = 140 Ω) connected between the probe and the cathode. The ion signal was registered by measuring the probe voltage (V_p) on R_1 using a resistive voltage divider (R_2 = 1 kΩ and R_3 = 12 Ω) with an input

resistance value much larger than the R_1 value but with a measuring resistance (R_3) small enough to avoid distortions of the signal due to the discharge of the 500 pF capacitor (corresponding to the measuring coaxial cable) on R_3. This biasing method takes advantage of the voltage distribution occurring during the arc discharge, and was successfully employed in a previous work [6]. To perform probe floating voltage measurements (with respect to the grounded anode), V_f, the values of R_2 and R_3 were changed to R_2 = 56 kΩ and R_3 = 3.3 kΩ, while R_1 was disconnected and the voltage on R_3 was registered (see Fig. 1). The discharge time of the 500 pF capacitor on the last R_3 value was short enough to avoid signal distortions in floating conditions. The employed oscilloscope was a two-channel Tektronix TDS 1002 B with a sampling rate of 500 MS/s, analogical bandwidth of 60 MHz, and an input impedance of 1 MΩ in parallel with a stray capacitance of 20 pF.

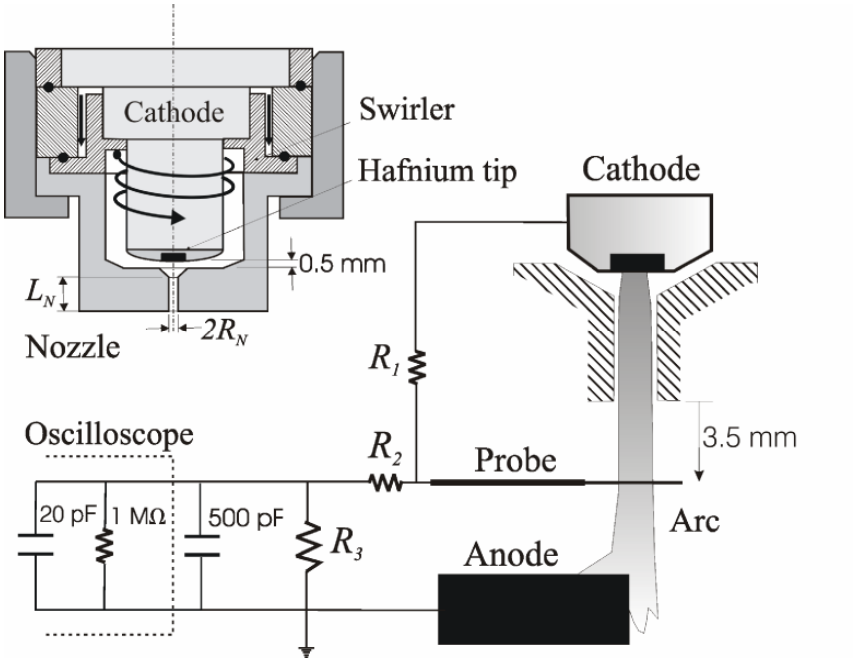

Figure 1. Scheme of the arc torch indicating several geometric dimensions**.** The probe biasing circuit is also shown.

3. Experimental Results

In Fig. 2 two typical probe ion current waveforms corresponding to nozzles of L_N = 4.5 mm operated at 0.7 MPa and L_N = 9.0 mm operated at 1.1 MPa are presented. The waveforms correspond to different arc runs, but for comparative purposes they were plotted on a single time scale. The registered gas flow rate trough the shorter nozzle was 35 Nl/min whereas only 20 Nl/min was measured for the larger nozzle in spite of its high operating pressure. As can be seen, both signals show an almost square shape but with differences in amplitude and time duration. For the nozzle with L_N = 4.5 mm a signal duration of ~ 50 μs (corresponding to an arc diameter of ~ 0.9 mm) and an ion current amplitude of ~ 0.8 A was registered. For the nozzle with L_N = 9.0 mm a signal duration of ~ 70 μs (corresponding to an arc diameter of ~ 1.3 mm) and an ion current amplitude of ~ 1.3 A was registered. The signal duration refers to the temporal width at the top of the flat-top profiles.

The total arc voltage, the nozzle voltage and the probe floating potential signals (measured at z = 3.5 mm from the nozzle exit in each case) were also measured (see Table 1). Note that the increase in the nozzle length leads to a substantially arc voltage rise (of about 55 V) corresponding to an arc power rise of about 1.65 kW. Statistical fluctuations in the current amplitude of the registered signals were ~ 5 %. The origin of such fluctuations is likely due to arc voltage fluctuations (ripple) that in turn produce corresponding changes in the plasma arc structure.

Table 1. Voltage measurements in the studied nozzles

	L_N = 4.5 mm	L_N = 9.0 mm
V_{CA} (V)	-160 ± 8	-215 ± 11
V_{NA} (V)	-80 ± 4	-95 ± 5
V_f (V)	-22 ± 1	-12 ± 0.6

No noticeable double-arcing damages were registered with the larger nozzle, in spite of the relatively small operating gas mass flow for this case.

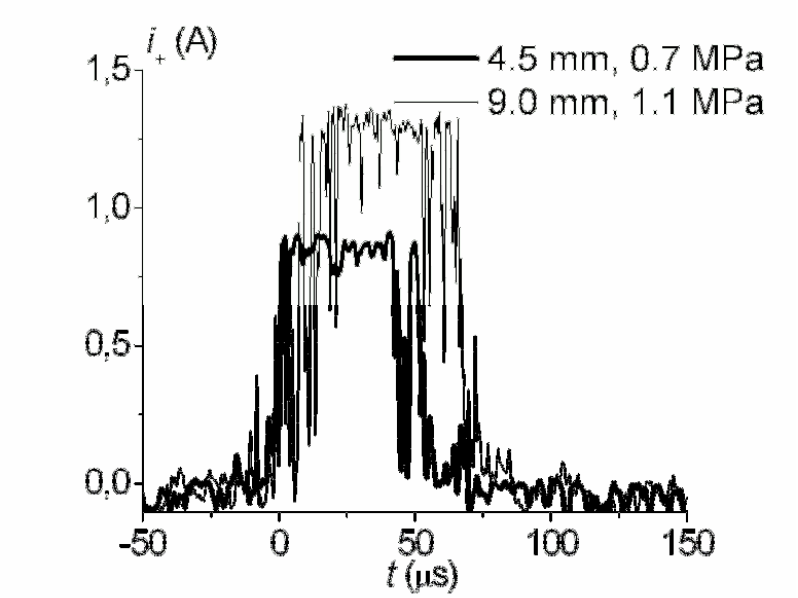

Figure 2. Typical probe ion signals obtained at 3.5 mm from the nozzle exit for the two nozzle lengths.

4. Interpretation of the results

The plasma is assumed in local thermodynamics equilibrium (LTE). Although the effects of non-LTE have been studied in cutting torches [5, 7] a theory based on LTE can in general give satisfactory temperature predictions when compared with experiments [1].

Assuming circular symmetry for the arc section, the arc core can be divided into several concentric elemental annulus (see Fig. 3)**,** so that the ion probe current can be expressed as the sum of contributions from many regions with different plasma quantity values, but at the same probe potential $V_p(x)$; where $x \equiv v_p\, t$ is the coordinate of the probe axis at a generic time t. As the electron thermal velocity $\bar{v}_e \equiv \sqrt{8kT/\pi m}$ (k is the Boltzmann's constant, T is the plasma temperature and m is the electron mass) is very large compared to the fluid-plasma velocity, the usual expression for the electron current collected by a probe in high-pressure quiescent plasmas applies. This current (per-unit probe length) for a cylindrical probe is [8]

$$i'_- = 2\pi R_p \frac{1}{\gamma}\frac{e\, n_e\, \bar{v}_e}{4}\exp\left(-\frac{e\left|V_p(x)-V_s\right|}{kT}\right) \qquad (1)$$

where e is the electron charge modulus, n_e the electron density, V_s the plasma potential and the non-dimensional correction factor γ is given by [8] $\gamma \approx 1+\frac{\lambda_D}{2\lambda_{ea}}\frac{kT}{e\left(V_f-V_s\right)}$, where λ_D is the electron Debye

length and λ_{ea} the electron mean free path for collisions with neutrals. The factor γ is very close to unity for the considered conditions ($\lambda_D << \lambda_{ea}$ and $kT/e < |V_p - V_s|$) and so $\gamma = 1$ was taken. The ion current (per-unit length) for a cylindrical probe in high-pressure high-velocity plasma jet, is given by [9]

$$i'_+ = 0.46\ e\, n_i v_B \lambda_{ia} \frac{e|V_p(x) - V_s|}{k\,T} \tag{2}$$

where n_i is the ion density, $v_B \equiv \sqrt{kT/M}$ the Bohm velocity (M is the ion mass) and λ_{ia} the ion mean free path for collisions between ions and neutrals, defined as $\lambda_{ia} \equiv 1/n_n\sigma_0$; where n_n is the neutral density and σ_0 is the elastic cross section, typically $\approx 5\times10^{-19}\ m^2$ [10].

The plasma potential value V_s can be obtained equating (1) and (2) for $V_p = V_f$,

$$0.18\sqrt{\frac{m}{M}}\frac{\lambda_{ia}}{R_p}\frac{e|V_f - V_s|}{kT} = \exp\left(-\frac{e|V_f - V_s|}{k\,T}\right). \tag{3}$$

From (3) and for the temperature range of interest $(10 \div 16)\,kK$ it results $V_s - V_f \approx 8\,V$.

Taking into account (2), and using simple geometrical considerations, the total ion current to the probe in terms of an integral along the radial direction is given by,

$$i_+\left(x \equiv v_p\, t\right) = 2\times0.46\ e \int_{r=|x|}^{R_A} \frac{|V_p(x) - V_s|}{k/e}\frac{n_i\, v_B\, \lambda_{ia}}{T}\frac{r}{\sqrt{r^2 - x^2}}\,dr \ . \tag{4}$$

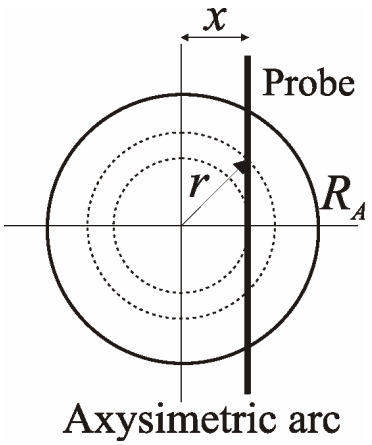

Figure 3. Scheme of the probe sweeping across the plasma at a generic time.

By using the Abel inversion technique, a radial profile of the plasma quantities can be derived from (4) with some additional assumptions. Note that the neutral density and the plasma density and temperature are involved in the integral appearing in (4). These magnitudes can be related through the state equation (assuming that the arc pressure is uniform along the radius) and through the Saha equation, thus closing the system. It is well known that any error in the input data for an Abel inversion technique can be amplified in the computation, and care must be taken to reduce such errors to a minimum. To this end, the input data were fitted with a high-order polynomial before performing the Abel inversion. The radial temperature and plasma charge density profiles were then calculated in accord with the Saha equilibrium and the ideal gas state equation for p = 0.13 MPa. The overpressure value of 0.03 MPa takes into account stagnation effects at the upstream edge of the probe surface for a plasma flow velocity of $\approx 2\times10^3$ m s^{-1} (of the order of the ion sound velocity) and a plasma density

corresponding to a pressure of 0.1 MPa and a temperature of 14 kK (as it will be shown later, this is a typical value obtained for *T*).

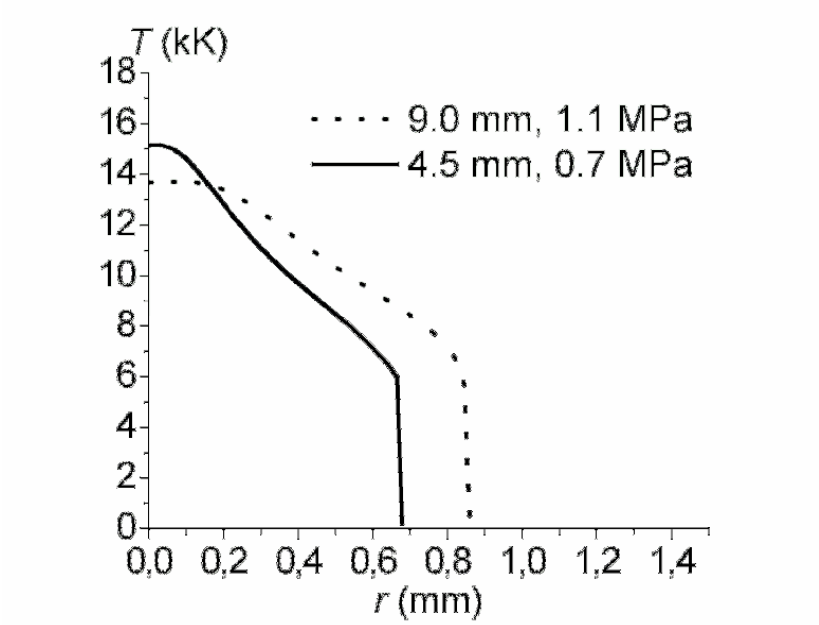

Figure 4. Radial profile of the plasma temperature obtained at 3.5 mm from the nozzle exit for the two nozzle lengths.

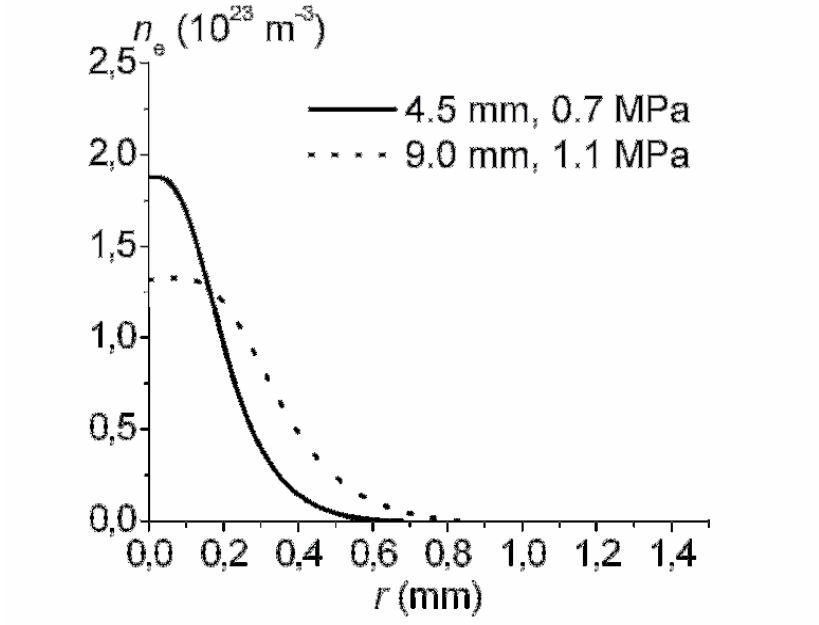

Figure 5. Radial profile of the plasma density obtained at 3.5 mm from the nozzle exit for the two nozzle lengths.

In Figs. 4 and 5 the obtained profiles of the plasma temperature and density are respectively shown for both nozzle geometries. As can be seen, the temperature profiles show a monotonic decrease from the arc center, and with a peak value (T_0) somewhat higher for the shorter nozzle ($T_0 \approx 15$ kK, whereas

$T_0 \approx 14$ kK for the larger nozzle). Also, the shorter nozzle produce a thinner arc (the profile decays abruptly at ≈ 0.7 mm, whereas the corresponding to the larger nozzle at ≈ 0.85 mm). It is worth noting that the abrupt decay at the end of the profiles cannot be taken with confidence as it is an artifact of the Abel inversion technique [11]. The plasma density profiles shown in Fig. 5 are obtained from the temperature profiles (Fig. 4) by applying the Saha equation. As expected, the larger density values are concentrated in the high temperature (T > 10 kK) region, and correspondingly, the peak value for the shorter nozzle is higher than that of the larger one. This behavior is attributed to the marked difference of gas flow rate due to the clogging effect. A low gas mass flow reduces the convective cooling at the arc border and decreases the radial heat flux, producing a decrease in the temperature drop from the arc axis. Due to the very strong dependence of the electrical conductivity on T (at 5 ÷ 10 kK), such decrease in the temperature drop results in a thicker arc with smaller axis temperature.

5. Final remarks

In this work, an experimental study on the influence of the nozzle geometry on the physical properties of a cutting arc is reported. Ion current signals collected by an electrostatic probe sweeping across a 30 A oxygen cutting arc at 3.5 mm from the nozzle exit for different nozzle lengths were registered. The temperature and density radial profiles of the arc plasma were found in each case by an inversion procedure of these signals. A comparison between the obtained results shows that the shorter nozzle (R_N = 0.50 mm, L_N = 4.5 mm operated at 0.7 MPa) produces a thinner and hotter arc than the larger nozzle (R_N = 0.50 mm, L_N = 9.0 mm operated at 1.1 MPa). This behavior is attributed to the marked difference of gas flow rate due to the clogging effect. A low gas mass flow reduces the convective cooling at the arc border and decreases the radial heat flux, producing a decrease in the temperature drop from the arc axis. Due to the very strong dependence of the electrical conductivity on T at (at 5 ÷ 10 kK), such decrease in the temperature drop results in a thicker arc with smaller axis temperature.

Acknowledgements
This work was supported by grants from the Universidad de Buenos Aires (PID X111) CONICET (PIP 5378) and Universidad Tecnológica Nacional (PID UTN 25/Z012).

References

[1] Freton P, Gonzalez J J, Gleizes A, Camy Peyret F, Caillibotte G and Delzenne M 2002 *J. Phys. D: Appl. Phys.* **35** 115.
[2] Boulos M, Fauchais P and Pfender E 1994 *Thermal Plasmas, Fundamentals and Applications* Vol. 1 (Plenum Press).
[3] Ramakrishnan S, Gershenzon M, Polivka F, Kearny T N and Rogozinsky M W 1997 *IEEE Trans. Plasma Sci.* **25** 937.
[4] Nemchinsky V A and Severance W S 2006 *J. Phys. D: Appl. Phys.* **39** R423.
[5] Peters J, Heberlein J and Lindsay J 2007 *J. Phys. D: Appl. Phys.* **40** 3960.
[6] Prevosto L, Kelly H and Mancinelli B 2008 *IEEE Trans. Plasma Sci.* **36** 263.
[7] Ghorui S, Heberlein J and Pfender E 2007 *J. Phys. D: Appl. Phys.* **40** 1966.
[8] Raizer Y P 1991 *Gas Discharge Physics* (Berlin, Germany: Springer).
[9] Prevosto L, Kelly H and Minotti F O 2008 *IEEE Trans. Plasma Sci.* **36** 271.
[10] Anderson H L 1989 *A physicist's Desk Reference* Second edition. (New York: AIP).
[11] Gick A E F, Quigley M B C, and Richards P H 1973 *J. Phys. D: Appl. Phys.* **6** 1941.